JBC ACCELERATED COMMUNICATIONS

The orphan receptor GPR139 signals via $G_{q/11}$ to oppose opioid effects

Received for publication, June 10, 2020, and in revised form, June 22, 2020 Published, Papers in Press, June 23, 2020, DOI 10.1074/jbc.AC120.014770

Hannah M. Stoveken, Stefano Zucca, Ikuo Masuho, Brock Grill, and Kirill A. Martemyanov*

From the Department of Neuroscience, The Scripps Research Institute, Jupiter, Florida, USA

Edited by Henrik G. Dohlman

The interplay between G protein–coupled receptors (GPCRs) is critical for controlling neuronal activity that shapes neuromodulatory outcomes. Recent evidence indicates that the orphan receptor GPR139 influences opioid modulation of key brain circuits by opposing the actions of the μ-opioid receptor (MOR). However, the function of GPR139 and its signaling mechanisms are poorly understood. In this study, we report that GPR139 activates multiple heterotrimeric G proteins, including members of the $G_{q/11}$ and $G_{i/o}$ families. Using a panel of reporter assays in reconstituted HEK293T/17 cells, we found that GPR139 functions via the $G_{q/11}$ pathway and thereby distinctly regulates cellular effector systems, including stimulation of cAMP production and inhibition of G protein inward rectifying potassium (GIRK) channels. Electrophysiological recordings from medial habenular neurons revealed that GPR139 signaling via $G_{q/11}$ is necessary and sufficient for counteracting MOR-mediated inhibition of neuronal firing. These results uncover a mechanistic interplay between GPCRs involved in controlling opioidergic neuromodulation in the brain.

The mammalian brain features a staggering number of neuromodulatory systems that often converge on the same neurons and must be integrated and balanced through a system of opposing signaling and feedback mechanisms (1). Most neuromodulators act on G protein–coupled receptors (GPCRs), an extensive protein family that triggers responses by engaging second messenger systems and ion channels. GPCR signals are relayed through an array of heterotrimeric G proteins comprised of 16 Gα subunits (2). The G protein(s) activated by a GPCR dictates the nature of the signal by engaging specific downstream targets. Ultimately, neuronal responses are built from cross-talk between GPCRs engaged by neuromodulatory inputs (1, 3). Understanding the logic and mechanisms of this GPCR signaling coordination is critical yet poorly explored.

Recently, we uncovered a novel regulatory GPCR system that revolves around GPR139 antagonizing the μ-opioid receptor (MOR) (4). MOR couples to the $G_{i/o}$ class of heterotrimeric G proteins to inhibit production of second messenger cAMP and to activate G protein inwardly rectifying potassium (GIRK) channels (5). It has been heavily targeted therapeutically for its desirable analgesic effects (6–10). However, MOR activation also generates untoward euphoria that leads to dependence (5, 11, 12). Our initial examination of the intersection between MOR and GPR139 revealed that multiple aspects of MOR signaling were impinged by GPR139, which could be aided by a physical interaction between the receptors (4). For instance, GPR139 enhanced β-arrestin recruitment to activated MOR and moderated its coupling to GIRK channels (4). However, the exact mechanism(s) of how GPR139 exerts an inhibitory influence on MOR and its relevance to the regulation of neuronal responses remains unknown.

The biology and signaling mechanisms of GPR139 are also poorly understood. It is an orphan GPCR expressed in select circuits in the brain, most notably in the areas implicated in motivation and reward (13–15). Whereas the endogenous ligand for GPR139 is a lingering question, it has been shown to be activated by the amino acids L-Phe and L-Trp and the neuropeptide α-MSH (13, 16, 17). Additionally, several synthetic ligands can activate GPR139 with high efficiency (18–20). Studies have also shown that GPR139 engages a variety of second messenger pathways when studied in transfected cells (14, 15, 21). However, its coupling to individual G proteins and their role in propagating downstream signals has not been holistically examined, which limits our understanding of the MOR-GPR139 interplay.

Here, we present the results of a systematic investigation of G protein–coupling selectivity of GPR139 and its role in signaling to downstream effectors. We also explore how GPR139 regulates MOR effects in a native neuronal setting. We establish that the key effects of GPR139 are mediated by $G_{q/11}$ signaling, which opposes the transmission of MOR signals at several intersecting points. Based on our findings, we propose that GPR139 "tunes" cellular responses to modulate opioid effects.

Results

GPR139 preferentially couples to $G\alpha_{11/q}$ and $G\alpha_{i/o}$

To determine the signaling properties of GPR139, we first examined its complete G protein–coupling profile. We used a bioluminescence resonance energy transfer (BRET) GPCR "fingerprinting" approach that permits the comprehensive study of unmodified receptors and unmodified Gα proteins to examine their coupling selectivity (22). In this assay, Venus-tagged $G\beta_1\gamma_2$ was paired with the nanoluciferase-based sensor mas-GRK3CT. In the presence of a chosen Gα subunit, GPCR activation triggers dissociation of the G protein heterotrimer, generating the BRET signal (Fig. 1*A*). Using this strategy, we surveyed GPR139 activity on 15 Gα proteins (Fig. 1, *B–F*) and recorded both the maximum amplitude and initial activation kinetics for each G protein (Fig. 1, *G* and *H*).

This article contains supporting information.

* For correspondence: Kirill A. Martemyanov, kirill@scripps.edu.

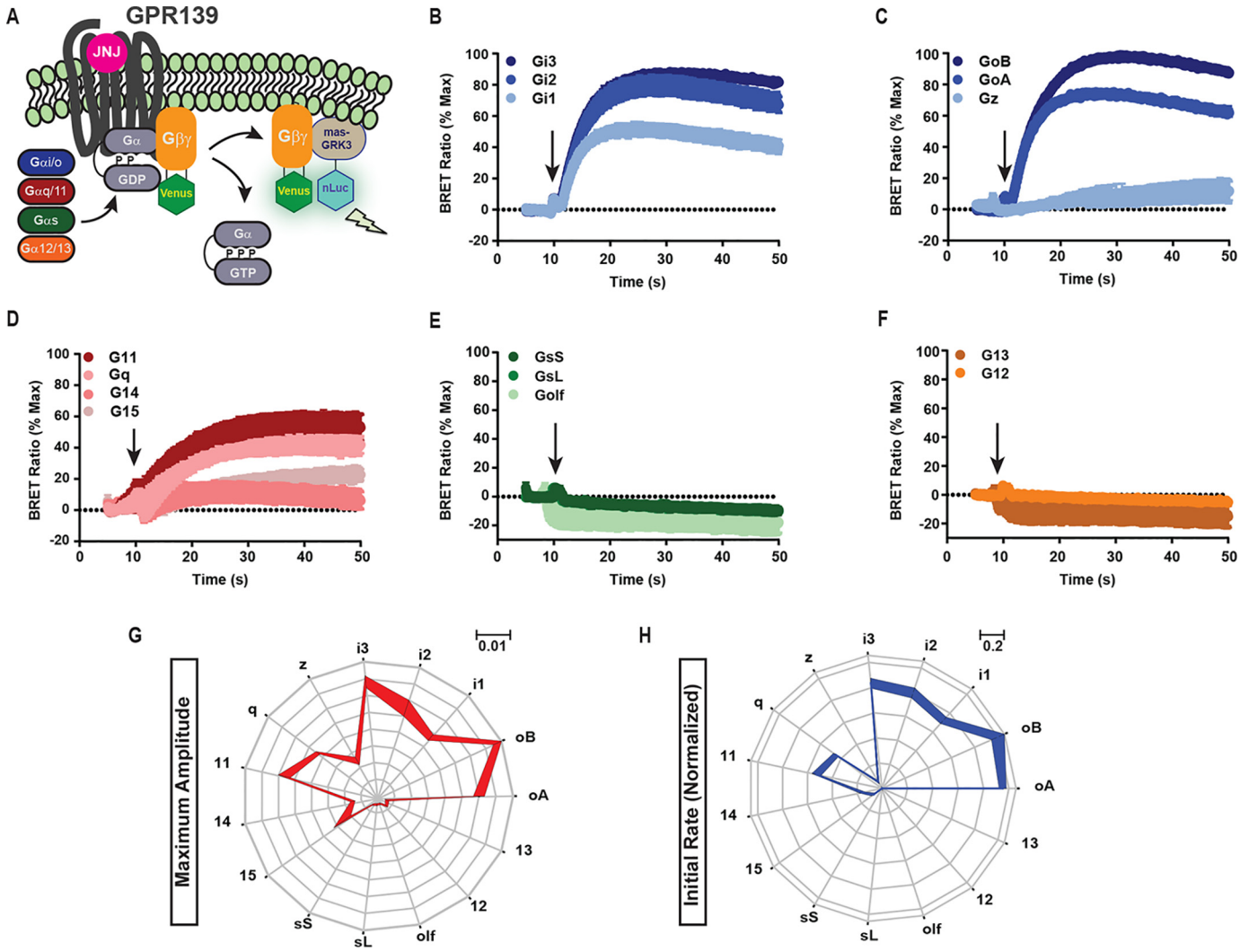

Figure 1. GPR139 G protein–coupling profile. *A*, schematic representation of the G protein BRET fingerprinting assay in HEK293 cells. *B–F*, GPR139 activity on the $G_{i/o}$ class (*B* and *C*), $G_{q/11}$ class (*D*), G_s class (*E*), or $G_{12/13}$ class (*F*) of G proteins. Amplitude and rate of activation were measured upon application of 10 μM JNJ-63533054, indicated by an *arrow*. Shown are the maximum amplitude (*G*) and the initial activation rate (*H*) for each G protein by GPR139. *A–F*, data are mean ± S.E. (*error bars*) of three independent experiments. *G* and *H*, mean of representative data ± S.D.

Interestingly, GPR139 could activate multiple G proteins with varying efficacies and kinetics. Within the $G_{i/o}$ class, there were no strong preferences for individual subtypes (Fig. 1, *B* and *C*). Within the $G_{q/11}$ class, only G_q and G_{11} showed appreciable activation (Fig. 1*D*). Dose-response studies with representative members further confirmed similar potencies of GPR139 coupling to G_{11} and G_o (Fig. S1). G_s and $G_{12/13}$ classes were not activated by GPR139 (Fig. 1, *E* and *F*). Side-by-side comparison of maximum amplitudes (Fig. 1*G*) and the activation rates (Fig. 1*H*) across all classes of G proteins revealed a unique fingerprint-like profile of GPR139 coupling preferences. Together, these results indicate that GPR139 is a dual-specificity receptor capable of activating G proteins of the $G_{i/o}$ and $G_{q/11}$ classes.

GPR139 selectively utilizes $G_{q/11}$ but not $G_{i/o}$ for signaling to downstream effectors

Because GPR139 can activate multiple G protein classes, which can lead to different cellular responses, we examined the effectors engaged by GPR139. We used a panel of sensors to assay the effect of GPR139 activation on Ca^{2+} mobilization, ion channel regulation, and cAMP generation (Fig. 2*A*).

When calcium levels were assayed with the BRET-based sensor CalFluxVTN (23), we observed that GPR139 activation triggered a rapid and transient increase in BRET signal (Fig. 2*B*) suggestive of Ca^{2+} release from intracellular stores and consistent with previous reports (14, 15). The application of the $G\alpha_q$ family–selective inhibitor YM-254890 completely blocked the response, indicating that the signal was mediated by $G\alpha_q$-type proteins (Fig. 2*B*). Dose-response studies confirmed these observations and established an EC_{50} of 75 ± 29 nM (Fig. 2*C*), which is consistent with the EC_{50} for G_{11} activation in the G protein BRET assay (119 ± 32 nM) (Fig. S1).

Next, we tested the influence of GPR139 on GIRK channels, which are activated by $G\beta\gamma$ released preferentially by $G_{i/o}$ proteins (24–26) (Fig. 2, *D* and *E*). We monitored GIRK channel opening kinetically by measuring thallium influx with an indicator dye (27). The simultaneous addition of thallium and the

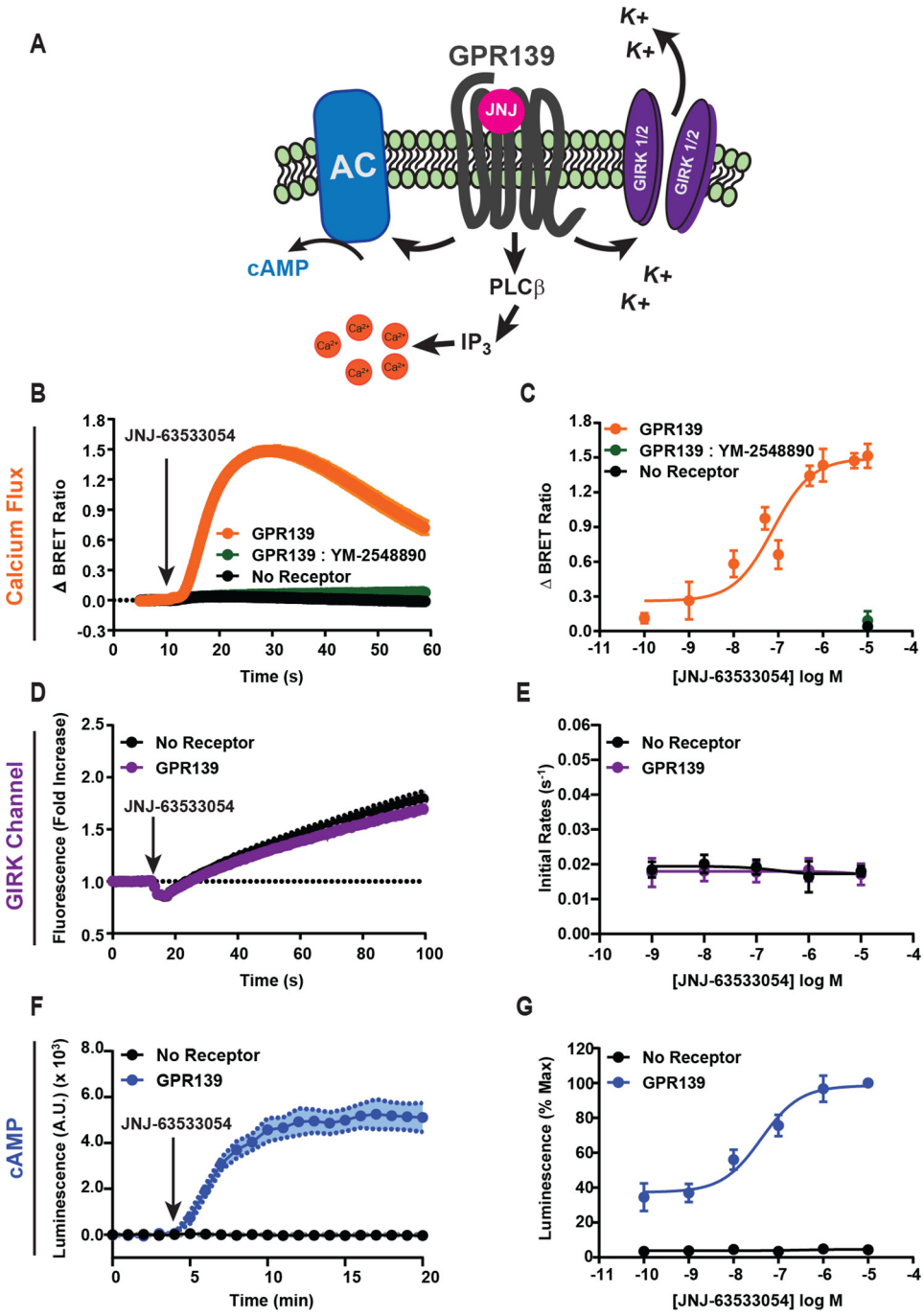

Figure 2. GPR139 signaling to downstream effectors. *A*, schematic of downstream signaling pathways examined. *B*, calcium mobilization was measured using the CalFluxVTN calcium biosensor in response to treating HEK293 cells with 10 μM JNJ-63533054. *C*, the maximal amplitude of the Ca^{2+} signal across concentrations of JNJ-63533054. *D*, thallium flux through GIRK1/2 channels in HEK293 cells upon treatment with 10 μM JNJ-63533054. *E*, the initial activation rate of thallium flux calculated across doses of JNJ-63533054. *F*, time course of GPR139 influence on cAMP. *G*, dose dependence of GPR139 activation on cAMP modulation. Data are mean ± S.E. (*error bars*) of 3–4 independent experiments.

GPR139 agonist JNJ-63533054 did not increase the rate of thallium influx compared with the slow, passive entry observed in cells without receptor (Fig. 2*D*). Dose-response studies quantifying changes in the slope of fluorescence showed no JNJ-63533054–induced changes at any concentration tested, confirming that GPR139 does not activate GIRK channels (Fig. 2*E*). Positive control experiments with MOR-transfected cells treated with morphine significantly increased the rate of GIRK channel activation, indicating adequate assay sensitivity (Fig. S2, *A* and *B*).

Finally, we measured the effect of GPR139 on cAMP generation with a biosensor (Fig. 2*F*). Unexpectedly, we found that GPR139 stimulation dynamically increased cAMP levels. The increase occurred in a dose-dependent manner with an EC_{50} of 41 ± 20 nM (Fig. 2*G*). GPR139 expression without agonist stimulation also increased the baseline cAMP levels, suggesting a

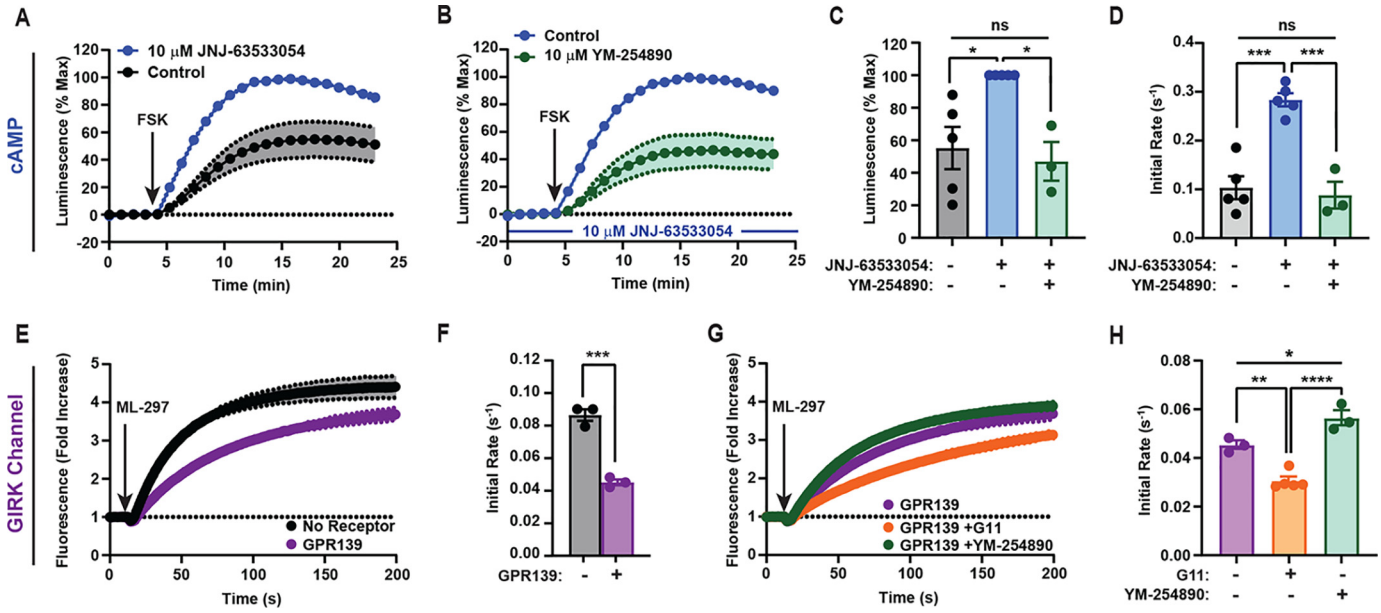

Figure 3. GPR139 signals selectively through $G_{q/11}$ to secondary effectors in cultured cells. Shown are changes in forskolin-stimulated cAMP (*A–D*) or ML-297-mediated GIRK1/2 activation (*E–H*) in response to GPR139 activation. *A*, effect of JNJ-63533054 on FSK-stimulated cAMP response. *B*, effect of pretreatment with G_q inhibitor YM-254890 on GPR139-mediated cAMP modulation. *C* and *D*, quantification of the maximum amplitude (*C*) and the initial activation rates (*D*) from *A* and *B*. *E*, effect of GPR139 on thallium flux through GIRK1/2 channels activated by ML-297. *F*, quantification of the initial activation rates from *E*. Student's *t* test was used: ***, $p < 0.001$. *G*, thallium flux in GPR139-expressing cells either additionally expressing G_{11} or pretreated with 10 μM YM-254890. *H*, quantification of the initial activation rates from *G*. Data are mean ± S.E. (*error bars*) of 3–5 independent experiments. *C*, *D*, and *H*, one-way analysis of variance with Tukey's post hoc test: *ns*, not significant; *, $p < 0.05$; **, $p < 0.01$; ***, $p < 0.001$; ****, $p < 0.0001$. *Shaded areas* in A, B, E, and G are S.E.

high level of constitutive activity (Fig. S3). In summary, these results indicate that GPR139 coupling to $G_{q/11}$ propagates to engage the canonical Ca^{2+} release pathway. However, despite the efficient coupling of GPR139 to $G_{i/o}$ and no coupling to $G_{s/olf}$, we observed no GIRK channel activation and paradoxical increase in cAMP production.

GPR139 signals to secondary effectors adenylyl cyclase and GIRK channels via $G\alpha_{q/11}$

The seemingly contradictory results between G protein coupling and downstream modulation of cAMP warranted further investigation. First, we tested whether GPR139 can also alter cAMP dynamics after treatment with the AC activator forskolin (FSK). Preincubation with JNJ-63533054 had no effect on cAMP dynamics in control cells (Fig. S4), but in GPR139-transfected cells, we detected a substantial enhancement of cAMP generation in both the amplitude and the initial activation rate (Fig. 3, *A*, *C*, and *D*).

Intriguingly, several AC isoforms known to be expressed in HEK293T can be regulated by calcium generated downstream of $G_{q/11}$-coupled GPCRs (28–30). To test the hypothesis that the GPR139-mediated changes in cAMP were driven by $G_{q/11}$ signaling, we blocked $G\alpha_{q/11}$ with YM-254890 and found that it prevented GPR139-mediated augmentation of cAMP generation (Fig. 3*B*). The maximal response elicited by co-application of YM-254890 with JNJ-63533054 was decreased compared with cells treated with agonist alone and restored back to the control-treated condition (Fig. 3*C*). Moreover, YM-254890 also abolished the effect of JNJ-63533054 on the acceleration of cAMP production rate (Fig. 3*D*).

We next addressed the inability to detect GIRK channel activation by GPR139 despite its coupling to $G_{i/o}$ (25, 26, 31). Interestingly, GIRK channels have also been shown to be impacted by G_q signaling acting via PIP_2 and protein kinase C to inhibit channel activity (31–33). Thus, we hypothesized that GPR139 could negatively regulate GIRK channels via G_q to prevent channel opening in response to $G_{i/o}$ activation. To test this hypothesis, we activated GIRK directly by agonist ML-297 (34), which requires PIP_2 as a cofactor, making it sensitive to G_q-mediated modulation (34, 35). Indeed, expression of GPR139 inhibited GIRK channel opening to 52.3 ± 1.6% of control (Fig. 3, *E* and *F*). Overexpression of G_{11} enhanced this inhibition (Fig. 3, *G* and *H*). In contrast, blockade of $G_{q/11}$ by YM-254890 diminished the inhibitory effects of GPR139 (Fig. 3, *G* and *H*). These effects were selective for GPR139 as MOR had no impact on ML-297–mediated GIRK activation either upon overexpression of G_{11} or blockade of $G_{q/11}$ by YM-254890 (Fig. S5, *A* and *B*). We thus conclude that GPR139 negatively regulates GIRK channel opening by engaging the $G_{q/11}$ pathway, which predominates over stimulatory $G_{i/o}$ engagement.

GPR139 signaling via $G_{q/11}$ opposes MOR-mediated suppression of neuronal firing

We next sought to determine the relevance of GPR139-mediated $G_{q/11}$ signaling to counteracting MOR in the endogenous setting by examining spontaneous neuron firing in the medial habenula (mHb), where MOR and GPR139 are co-expressed (4, 36). Application of the MOR agonist DAMGO significantly dampened neuronal firing and reversed upon DAMGO washout (Fig. 4, *A*, *B*, and *D*). Pretreatment with JNJ-63533054 did not change the baseline firing rate (Fig. 4*A*) but

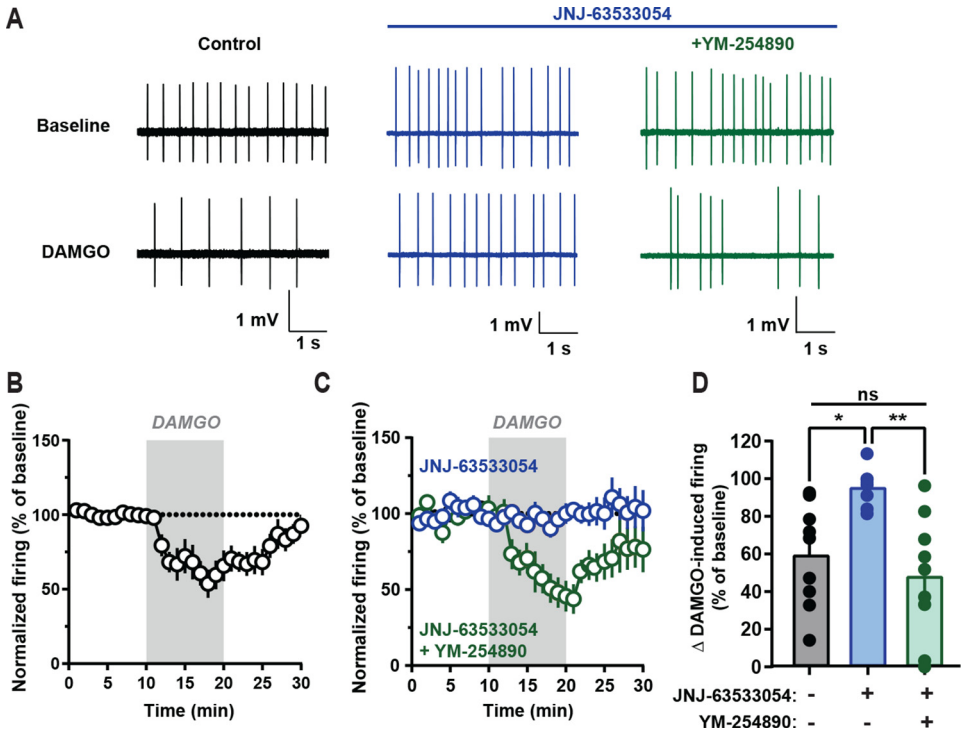

Figure 4. GPR139 signals via $G_{q/11}$ to oppose opioid-mediated inhibition of neuronal firing in medial habenula. *A*, representative firing traces recorded from medial habenular neurons in brain slices. *B* and *C*, change in firing frequency upon treatment with MOR agonist DAMGO. Slices were pretreated with vehicle (*B*) or 10 μM JNJ-63533054 (*blue trace*) (*C*) or with 10 μM JNJ-63533054 and 10 μM YM-254890 (*green trace*). *D*, maximum change in firing was quantified for (*B* and *C*). Data are mean ± S.E. of 8–10 neurons/trace; one-way analysis of variance with Tukey's post hoc test: *ns*, not significant; *, $p < 0.05$; **, $p < 0.01$.

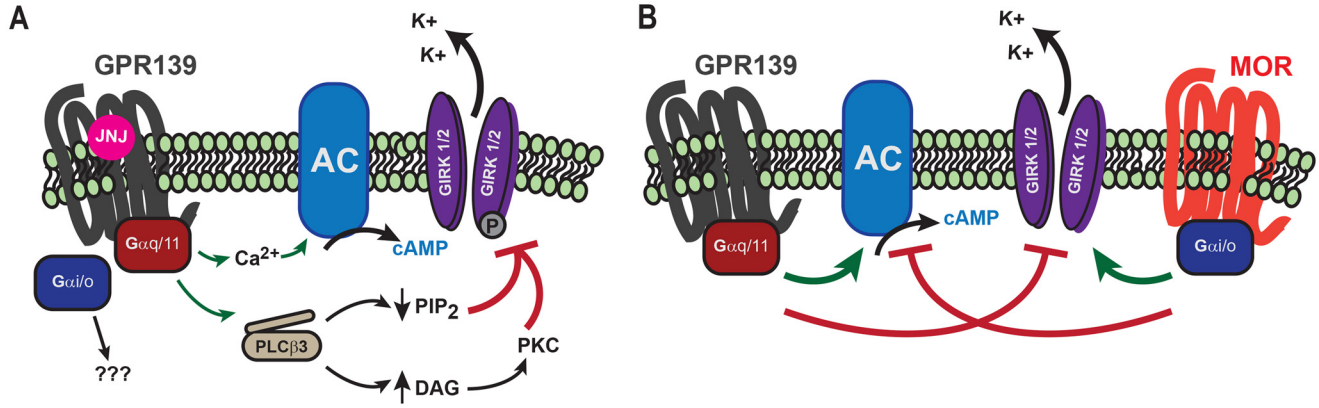

Figure 5. GPR139 signaling mechanisms. *A*, GPR139 activates both $G_{q/11}$ and $G_{i/o}$ classes of G proteins, but signaling to secondary effectors is mediated by $G_{q/11}$. *B*, GPR139 counteracts MOR signaling by opposing regulation of the downstream effectors AC and GIRK channels.

completely blocked DAMGO's effects on firing (Fig. 4, *A*, *C*, and *D*). This effect of JNJ-63533054 was specific as it did not block DAMGO influence on firing in *GPR139*$^{-/-}$ mice (Fig. S6, *A* and *B*). Importantly, blockade of $G\alpha_{q/11}$ with YM-254890 reversed the effects of the JNJ-63533054 and restored inhibition of firing in response to DAMGO (Fig. 4, *A*, *C*, and *D*). Taken together, these data indicate that GPR139-initiated $G_{q/11}$ signaling is sufficient to counteract MOR-mediated effects on mHb neuron firing.

Discussion

Orphan GPCRs comprise ~100 receptors with unknown ligands and often unknown physiological roles and signaling (37) yet critical involvement in many neuronal functions (38). Thus, elucidating their functional roles presents a compelling research frontier. GPR139 is an orphan GPCR with poorly understood biology and signaling mechanisms. It is an intriguing receptor for its selective expression pattern across brain circuits and involvement in movement (13) and the effects of alcohol and opioids (4, 39). We recently found that GPR139 is molecularly intertwined with MOR and opposes its signaling, offering the first glimpse of a possible physiological role for GPR139 in regulating reward (4). In this report, we provide critical insight into unanswered questions regarding GPR139 signaling mechanisms. We show that GPR139 primarily engages the $G_{q/11}$ pathway to activate adenylyl cyclase and inhibit the GIRK channel, key effector molecules that are regulated in an

opposite fashion by MOR, thereby providing a mechanistic basis for the signaling cross-talk (Fig. 5). We further show that this $G_{q/11}$-mediated signaling is essential for GPR139's ability to inhibit opioid effects in mHb neurons. The $G_{q/11}$ mechanism identified in this study may complement the direct inhibitory effects of GPR139 on MOR mediated by heterologous β-arrestin recruitment and heteromerization reported previously (4).

Our observations that GPR139 effectively utilizes $G_{q/11}$ to suppress MOR signaling mediated by $G_{i/o}$ provides a clear illustration of the signaling cross-talk that occurs at the level of G proteins competing to regulate common effectors. The interplay between $G_{q/11}$ and $G_{i/o}$ has been noted for ion channels and adenylyl cyclase (40, 41). In particular, opposing signaling between $G\alpha_q$ and $G\alpha_o$ pathways has been well-documented in *Caenorhabditis elegans* (42–44). On the other hand, $G_{i/o}$-coupled receptors may act synergistically with $G_{q/11}$-coupled receptors to potentiate $G_{q/11}$-mediated signaling (45–47). Thus, the cellular context likely affects whether $G_{q/11}$ and $G_{i/o}$ display an inhibitory or synergistic relationship. Therefore, the full extent of MOR-GPR139 cross-talk is likely more nuanced and context-dependent, making it possible that regulation of effector systems may vary in different neuronal populations. We envision that $G_{q/11}$ signaling by GPR139 may also similarly interfere with the $G_{i/o}$ signals generated by other GPCRs co-expressed with GPR139. Such a scenario and the possible range of additional $G_{i/o}$-coupled GPCR targets impacted by GPR139 remains to be established. From this perspective, it is intriguing that a recent study reported a possible functional interaction between GPR139 and the $G_{i/o}$-coupled dopamine 2 receptor (48). The interplay of GPR139 with other GPCRs may differ from what we observe for MOR and may be shaped by heteromerization, compartment localization, and cellular environment.

Our exhaustive profiling of G protein coupling revealed that GPR139 can activate multiple G proteins. Whereas this study establishes the role of the $G_{q/11}$ branch in mediating GPR139 effects on opioid signaling, the relevance and roles of other signaling modalities remain to be determined. It seems possible that other Gα species may fine-tune GPR139 effects or allow it to access different signaling modalities. We are intrigued by the robust coupling of GPR139 to the $G_{i/o}$ class. This coupling does not result in the engagement of typical $G_{i/o}$ effectors, likely due to antagonism from $G\alpha_q$ that overpowers it, yet $G_{i/o}$ is expected to be concurrently activated. We envision two potential mechanisms that could exploit this dual coupling. First, concurrent activation of $G_{i/o}$ may serve to constrain the $G_{q/11}$ signals endowing GPR139 with a self-pacing mechanism. Second, $G_{i/o}$ signaling might be preferentially realized in some neuronal populations where the $G_{q/11}$ branch is weak. This would enable bidirectional control of cellular signaling by GPR139, depending on the G protein contingent in a given neuron. In any event, the complete map of G protein selectiveness presented in this study should enable exploration of GPR139 signaling modalities in future studies.

One key frontier in GPR139 research is related to its activation mechanism. We observed GPR139 activity in the absence of agonist in every assay performed, which likely reflects high constitutive activity. GPR139 could use this constitutive inhibitory influence to dampen or enhance the response of MOR to endogenous opioid peptides. In addition, GPR139 could also be modulated by ligands. The amino acids L-Phe and L-Trp have been reported to activate GPR139 with an EC_{50} in the 200–300 μM range (16). These amino acids are present in the culture media at a ~20–70 μM range and thus may enhance GPR139 activity. GPR139 could also be activated by several peptides, most prominently α-MSH, although there are conflicting reports (17, 49). Whether these peptides are involved in mediating GPR139 modulation of opioid signaling in endogenous neural circuits remains to be established.

Our observations suggest a strategy for increasing the therapeutic window of opioids. We predict that GPR139 antagonists and/or inverse agonists would be useful to enhance the behavioral sensitivity to opioids. Several groups have performed high-throughput screens to identify potential antagonists, but most compounds identified exhibit low potency and poor specificity and are therefore of limited utility for *in vivo* applications (21, 50). Discrete distribution of GPR139 in the brain, its robust anti-opioid activity, and the demonstration of its signaling mechanisms presented in this paper makes this orphan receptor an attractive therapeutic target.

Experimental procedures

Reagents and constructs

Dulbecco's modified Eagle's medium, Opti-MEM, sodium pyruvate, Lipofectamine 3000, nonessential amino acids, and Hanks' balanced saline solution with Ca^{2+} and Mg^{2+} were purchased from Invitrogen (Carlsbad, CA). Matrigel was from Corning Life Sciences. NanoGlo Luciferase Reagent, GloSensor cAMP reagent, and the pGloSensor −22F cAMP plasmid were purchased from Promega Corp. (Madison, WI). (S)-JNJ-63533054 was synthesized as described (18). YM-254890 was purchased from Wako Chemicals USA, Inc. (Richmond, VA). The GPR139 cDNA used for all experiments (HASP-HA-GPR139) contained an N-terminal HA signal peptide (HASP), followed by an HA tag and human GPR139 (NM_001002911.4).

Cell culture and transfection

HEK293T/17 cells were maintained in Dulbecco's modified Eagle's medium + 10% (v/v) fetal bovine serum, nonessential amino acids, and 1 mM sodium pyruvate. Transfections were performed as described (51).

G protein BRET assay

HEK293T/17 cells were transfected with HASP-HA-GPR139 pcDNA3.1 and 0.84 μg of $G\alpha_o$ pcMV5, 0.84 μg of $G\alpha_{11}$ pcDNA3.1, or 0.84 μg of the indicated Gα protein. Additionally, 0.42 μg of Venus(1–155)-Gγ2 pcDNA3.1, 0.42 μg of Venus (156–299)-Gβ1 pcDNA3.1, and 0.42 μg of mas-GRK3-NanoLuc pcDNA3.1 were transfected, and DNAs were balanced to 10 μg using pcDNA3.1 and assays were performed as described (22).

CalFluxVTN calcium assay

HEK293T/17 cells were transfected with 0.84 μg of HASP-HA-GPR139 pcDNA3.1 and 0.84 μg of CalFluxVTN pcDNA3.1 and incubated overnight, and the assay was performed as

described (52), measuring luminescence every 0.06 s using the PHERAstar FSX plate reader.

−22F pGLO assay

HEK293T cells were transfected using 0.42 μg of HASP-HA-GPR139 pcDNA3.1, 0.21 μg of MOR-FLAG, and 0.42 μg of −22F pGloSensor™ cAMP plasmid. The next day, cells were reseeded in a 96-well plate in culture medium at 1×10^5 cells/well for 2 h at 37 °C and 5% CO_2. The overlaying medium was then replaced with 40 μl of 1× GloSensor™ cAMP reagent and measured as described (53).

Thallium flux

GIRK channel function was assessed using the Molecular Devices FLIPR® potassium assay kit. The following cDNAs were transfected: 0.84 μg of MOR-FLAG pcDNA3.1, 0.21 μg of HASP-HA-GPR139 pcDNA3.1, 1.26 μg of GIRK-1-AU5 pCMV5, 1.26 μg of mGIRK-2a pCMV5, 0.84 μg of rat Gαo pCMV, 0.42 μg of Gβ1 pcDNA3.1, 0.42 μg of Gγ2 pcDNA3.1, and for the indicated assay conditions, 0.42 μg of hGα11 pcDNA3.1. Cells were incubated for 18–24 h at 37 °C and 5% CO_2. The next day, cells were reseeded at 20,000 cells/well of a black 384-well Corning CellBIND® plate and treated with or without 10 μM YM-254890. Cells were incubated for an additional 18–24 h. On the day of the experiment, 20 μl of loading buffer was added to 20 μl of cell culture per the manufacturer's instructions. Plates were incubated in the dark at room temperature for 1 h.

Baseline signaling was assessed for 10 reads at 1 s/read using the FLIPR Tetra®. Data were normalized as -fold over baseline, and the change in activation over time was compared by fitting a straight line to the data within the initial linear range of activation (15–25 s) using GraphPad Prism 8.

Slice electrophysiology

All procedures involving mice were approved by the institutional animal care and use committee at Scripps Research and were carried out in strict compliance with National Institutes of Health guidelines. Mice of either sex aged 2–4 months were anesthetized with isoflurane and decapitated. Brain slices were prepared, and loose-seal, cell-attached recordings from habenular neurons were performed as described (4). Changes in firing frequency following pharmacological treatments were quantified as the mean value of the last 3 min of the recordings in the presence of the drug, normalized with respect to the last 3 min of baseline preceding the drug application. Current clamp signals were high pass–filtered at 300 Hz.

Data availability

Any data not in the article can be shared upon request.

Acknowledgments—We thank Natalia Maremyanova for mouse husbandry and Nickolas K. Skamangas for technical support.

Author contributions—H. M. S. and K. A. M. conceptualization; H. M. S. data curation; H. M. S., S. Z., and I. M. formal analysis; H. M. S., S. Z., and I. M. investigation; H. M. S. and K. A. M. writing-original draft; H. M. S., S. Z., I. M., B. G., and K. A. M. writing-review and editing; B. G. resources; B. G. and K. A. M. funding acquisition; K. A. M. supervision; K. A. M. project administration.

Funding and additional information—This work was supported by National Institutes of Health Grants DA036596 (to K. A. M.), DA048036 (to B. G. and K. A. M.), DA047771 (to H. M. S.), and DA048579 (to S. Z.). The content is solely the responsibility of the authors and does not necessarily represent the official views of the National Institutes of Health.

Conflict of interest—B. G. and K. A. M. have filed a patent on the utility of GPR139 as a drug target.

Abbreviations—The abbreviations used are: GPCR, G protein–coupled receptor; AC, adenylyl cyclase; MOR, μ-opioid receptor; GIRK, G protein inward rectifying potassium; BRET, bioluminescence resonance energy transfer; FSK, forskolin; PIP_2, phosphatidylinositol 4,5-bisphosphate; mHb, medial habenula; HA, hemagglutinin; HASP, HA signal peptide.

References

1. Huang, Y., and Thathiah, A. (2015) Regulation of neuronal communication by G protein-coupled receptors. *FEBS Lett.* **589,** 1607–1619 CrossRef Medline
2. Milligan, G., and Kostenis, E. (2006) Heterotrimeric G-proteins: a short history. *Br. J. Pharmacol.* **147,** S46–S55 CrossRef Medline
3. Greengard, P. (2001) The neurobiology of slow synaptic transmission. *Science* **294,** 1024–1030 CrossRef Medline
4. Wang, D., Stoveken, H. M., Zucca, S., Dao, M., Orlandi, C., Song, C., Masuho, I., Johnston, C., Opperman, K. J., Giles, A. C., Gill, M. S., Lundquist, E. A., Grill, B., and Martemyanov, K. A. (2019) Genetic behavioral screen identifies an orphan anti-opioid system. *Science* **365,** 1267–1273 CrossRef Medline
5. Al-Hasani, R., and Bruchas, M. R. (2011) Molecular mechanisms of opioid receptor-dependent signaling and behavior. *Anesthesiology* **115,** 1363–1381 CrossRef Medline
6. Chen, Y., Mestek, A., Liu, J., Hurley, J. A., and Yu, L. (1993) Molecular cloning and functional expression of a μ-opioid receptor from rat brain. *Mol. Pharmacol.* **44,** 8–12 Medline
7. Matthes, H. W., Maldonado, R., Simonin, F., Valverde, O., Slowe, S., Kitchen, I., Befort, K., Dierich, A., Le Meur, M., Dollé, P., Tzavara, E., Hanoune, J., Roques, B. P., and Kieffer, B. L. (1996) Loss of morphine-induced analgesia, reward effect and withdrawal symptoms in mice lacking the μ-opioid-receptor gene. *Nature* **383,** 819–823 CrossRef Medline
8. Pert, C. B., and Snyder, S. H. (1973) Opiate receptor: demonstration in nervous tissue. *Science* **179,** 1011–1014 CrossRef Medline
9. Clark, M. J., Furman, C. A., Gilson, T. D., and Traynor, J. R. (2006) Comparison of the relative efficacy and potency of μ-opioid agonists to activate $G\alpha_{i/o}$ proteins containing a pertussis toxin-insensitive mutation. *J. Pharmacol. Exp. Ther.* **317,** 858–864 CrossRef Medline
10. Laugwitz, K. L., Offermanns, S., Spicher, K., and Schultz, G. (1993) μ and δ opioid receptors differentially couple to G protein subtypes in membranes of human neuroblastoma SH-SY5Y cells. *Neuron* **10,** 233–242 CrossRef Medline
11. Darcq, E., and Kieffer, B. L. (2018) Opioid receptors: drivers to addiction? *Nat. Rev. Neurosci.* **19,** 499–514 CrossRef Medline
12. Navratilova, E., Atcherley, C. W., and Porreca, F. (2015) Brain circuits encoding reward from pain relief. *Trends Neurosci.* **38,** 741–750 CrossRef Medline
13. Liu, C., Bonaventure, P., Lee, G., Nepomuceno, D., Kuei, C., Wu, J., Li, Q., Joseph, V., Sutton, S. W., Eckert, W., Yao, X., Yieh, L., Dvorak, C.,

Carruthers, N., Coate, H., *et al.* (2015) GPR139, an orphan receptor highly enriched in the habenula and septum, is activated by the essential amino acids L-tryptophan and L-phenylalanine. *Mol. Pharmacol.* **88,** 911–925 CrossRef Medline

14. Matsuo, A., Matsumoto, S., Nagano, M., Masumoto, K. H., Takasaki, J., Matsumoto, M., Kobori, M., Katoh, M., and Shigeyoshi, Y. (2005) Molecular cloning and characterization of a novel G_q-coupled orphan receptor GPRg1 exclusively expressed in the central nervous system. *Biochem. Biophys. Res. Commun.* **331,** 363–369 CrossRef Medline
15. Süsens, U., Hermans-Borgmeyer, I., Urny, J., and Schaller, H. C. (2006) Characterisation and differential expression of two very closely related G-protein-coupled receptors, GPR139 and GPR142, in mouse tissue and during mouse development. *Neuropharmacology* **50,** 512–520 CrossRef Medline
16. Isberg, V., Andersen, K. B., Bisig, C., Dietz, G. P., Bräuner-Osborne, H., and Gloriam, D. E. (2014) Computer-aided discovery of aromatic l-α-amino acids as agonists of the orphan G protein-coupled receptor GPR139. *J. Chem. Inf. Model.* **54,** 1553–1557 CrossRef Medline
17. Nøhr, A. C., Shehata, M. A., Hauser, A. S., Isberg, V., Mokrosinski, J., Andersen, K. B., Farooqi, I. S., Pedersen, D. S., Gloriam, D. E., and Bräuner-Osborne, H. (2017) The orphan G protein-coupled receptor GPR139 is activated by the peptides: adrenocorticotropic hormone (ACTH), α-, and β-melanocyte stimulating hormone (α-MSH, and β-MSH), and the conserved core motif HFRW. *Neurochem. Int.* **102,** 105–113 CrossRef Medline
18. Dvorak, C. A., Coate, H., Nepomuceno, D., Wennerholm, M., Kuei, C., Lord, B., Woody, D., Bonaventure, P., Liu, C., Lovenberg, T., and Carruthers, N. I. (2015) Identification and SAR of glycine benzamides as potent agonists for the GPR139 receptor. *ACS Med. Chem. Lett.* **6,** 1015–1018 CrossRef Medline
19. Nøhr, A. C., Shehata, M. A., Palmer, D., Pokhrel, R., Vallianou, M., Foster, S. R., Gentry, P. R., Gloriam, D. E., and Bräuner-Osborne, H. (2019) Identification of a novel scaffold for a small molecule GPR139 receptor agonist. *Sci. Rep.* **9,** 3802 CrossRef Medline
20. Shi, F., Shen, J. K., Chen, D., Fog, K., Thirstrup, K., Hentzer, M., Karlsson, J. J., Menon, V., Jones, K. A., Smith, K. E., and Smith, G. (2011) Discovery and SAR of a series of agonists at orphan G protein-coupled receptor 139. *ACS Med. Chem. Lett.* **2,** 303–306 CrossRef Medline
21. Hu, L. A., Tang, P. M., Eslahi, N. K., Zhou, T., Barbosa, J., and Liu, Q. (2009) Identification of surrogate agonists and antagonists for orphan G-protein-coupled receptor GPR139. *J. Biomol. Screen.* **14,** 789–797 CrossRef Medline
22. Masuho, I., Ostrovskaya, O., Kramer, G. M., Jones, C. D., Xie, K., and Martemyanov, K. A. (2015) Distinct profiles of functional discrimination among G proteins determine the actions of G protein-coupled receptors. *Sci. Signal.* **8,** ra123 CrossRef Medline
23. Yang, J., Cumberbatch, D., Centanni, S., Shi, S. Q., Winder, D., Webb, D., and Johnson, C. H. (2016) Coupling optogenetic stimulation with NanoLuc-based luminescence (BRET) Ca^{2+} sensing. *Nat. Commun.* **7,** 13268 CrossRef Medline
24. Breitwieser, G. E., and Szabo, G. (1985) Uncoupling of cardiac muscarinic and beta-adrenergic receptors from ion channels by a guanine nucleotide analogue. *Nature* **317,** 538–540 CrossRef Medline
25. Huang, C. L., Slesinger, P. A., Casey, P. J., Jan, Y. N., and Jan, L. Y. (1995) Evidence that direct binding of Gβγ to the GIRK1 G protein-gated inwardly rectifying K^+ channel is important for channel activation. *Neuron* **15,** 1133–1143 CrossRef Medline
26. Pfaffinger, P. J., Martin, J. M., Hunter, D. D., Nathanson, N. M., and Hille, B. (1985) GTP-binding proteins couple cardiac muscarinic receptors to a K channel. *Nature* **317,** 536–538 CrossRef Medline
27. Weaver, C. D., Harden, D., Dworetzky, S. I., Robertson, B., and Knox, R. J. (2004) A thallium-sensitive, fluorescence-based assay for detecting and characterizing potassium channel modulators in mammalian cells. *J. Biomol. Screen.* **9,** 671–677 CrossRef Medline
28. Atwood, B. K., Lopez, J., Wager-Miller, J., Mackie, K., and Straiker, A. (2011) Expression of G protein-coupled receptors and related proteins in HEK293, AtT20, BV2, and N18 cell lines as revealed by microarray analysis. *BMC Genomics* **12,** 14 CrossRef Medline
29. Beazely, M. A., and Watts, V. J. (2005) $Gα_q$-coupled receptor signaling enhances adenylate cyclase type 6 activation. *Biochem. Pharmacol.* **70,** 113–120 CrossRef Medline
30. Sadana, R., and Dessauer, C. W. (2009) Physiological roles for G protein-regulated adenylyl cyclase isoforms: insights from knockout and overexpression studies. *Neurosignals* **17,** 5–22 CrossRef Medline
31. Huang, C. L., Feng, S., and Hilgemann, D. W. (1998) Direct activation of inward rectifier potassium channels by PIP_2 and its stabilization by Gβγ. *Nature* **391,** 803–806 CrossRef Medline
32. Keselman, I., Fribourg, M., Felsenfeld, D. P., and Logothetis, D. E. (2007) Mechanism of PLC-mediated Kir3 current inhibition. *Channels (Austin)* **1,** 113–123 CrossRef Medline
33. Lei, Q., Talley, E. M., and Bayliss, D. A. (2001) Receptor-mediated inhibition of G protein-coupled inwardly rectifying potassium channels involves $Gα_q$ family subunits, phospholipase C, and a readily diffusible messenger. *J. Biol. Chem.* **276,** 16720–16730 CrossRef Medline
34. Kaufmann, K., Romaine, I., Days, E., Pascual, C., Malik, A., Yang, L., Zou, B., Du, Y., Sliwoski, G., Morrison, R. D., Denton, J., Niswender, C. M., Daniels, J. S., Sulikowski, G. A., Xie, X. S., *et al.* (2013) ML297 (VU0456810), the first potent and selective activator of the GIRK potassium channel, displays antiepileptic properties in mice. *ACS Chem. Neurosci.* **4,** 1278–1286 CrossRef Medline
35. Wydeven, N., Marron Fernandez de Velasco, E., Du, Y., Benneyworth, M. A., Hearing, M. C., Fischer, R. A., Thomas, M. J., Weaver, C. D., and Wickman, K. (2014) Mechanisms underlying the activation of G-protein-gated inwardly rectifying K^+ (GIRK) channels by the novel anxiolytic drug, ML297. *Proc. Natl. Acad. Sci. U. S. A.* **111,** 10755–10760 CrossRef Medline
36. Boulos, L. J., Darcq, E., and Kieffer, B. L. (2017) Translating the habenula: from rodents to humans. *Biol. Psychiatry* **81,** 296–305 CrossRef Medline
37. Sriram, K., and Insel, P. A. (2018) G protein-coupled receptors as targets for approved drugs: how many targets and how many drugs? *Mol. Pharmacol.* **93,** 251–258 CrossRef Medline
38. Alavi, M. S., Shamsizadeh, A., Azhdari-Zarmehri, H., and Roohbakhsh, A. (2018) Orphan G protein-coupled receptors: the role in CNS disorders. *Biomed. Pharmacother.* **98,** 222–232 CrossRef Medline
39. Kononoff, J., Kallupi, M., Kimbrough, A., Conlisk, D., de Guglielmo, G., and George, O. (2018) Systemic and intra-habenular activation of the orphan G protein-coupled receptor GPR139 decreases compulsive-like alcohol drinking and hyperalgesia in alcohol-dependent rats. *eNeuro* **5,** ENEURO.0153-18.2018 CrossRef Medline
40. Halls, M. L., and Cooper, D. M. F. (2017) Adenylyl cyclase signalling complexes: pharmacological challenges and opportunities. *Pharmacol. Ther.* **172,** 171–180 CrossRef Medline
41. Inanobe, A., and Kurachi, Y. (2014) Membrane channels as integrators of G-protein-mediated signaling. *Biochim. Biophys. Acta* **1838,** 521–531 CrossRef Medline
42. Bastiani, C., and Mendel, J. (2006) Heterotrimeric G proteins in *C. elegans*. *WormBook* 1–25 CrossRef Medline
43. Hajdu-Cronin, Y. M., Chen, W. J., Patikoglou, G., Koelle, M. R., and Sternberg, P. W. (1999) Antagonism between $G_oα$ and $G_qα$ in *Caenorhabditis elegans*: the RGS protein EAT-16 is necessary for $G_oα$ signaling and regulates $G_qα$ activity. *Genes Dev.* **13,** 1780–1793 CrossRef Medline
44. Miller, K. G., Emerson, M. D., and Rand, J. B. (1999) $G_oα$ and diacylglycerol kinase negatively regulate the $G_qα$ pathway in *C. elegans*. *Neuron* **24,** 323–333 CrossRef Medline
45. Gerwins, P., and Fredholm, B. B. (1992) Stimulation of adenosine A1 receptors and bradykinin receptors, which act via different G proteins, synergistically raises inositol 1,4,5-trisphosphate and intracellular free calcium in DDT1 MF-2 smooth muscle cells. *Proc. Natl. Acad. Sci. U. S. A.* **89,** 7330–7334 CrossRef Medline
46. Seyedi, N., Win, T., Lander, H. M., and Levi, R. (1997) Bradykinin B2-receptor activation augments norepinephrine exocytosis from cardiac sympathetic nerve endings: mediation by autocrine/paracrine mechanisms. *Circ. Res.* **81,** 774–784 CrossRef Medline
47. Shah, B. H., Siddiqui, A., Qureshi, K. A., Khan, M., Rafi, S., Ujan, V. A., Yakoob, M. Y., Yaqub, Y., Rasheed, H., and Saeed, S. A. (1999) Co-

activation of G_i and G_q proteins exerts synergistic effect on human platelet aggregation through activation of phospholipase C and Ca^{2+} signalling pathways. *Exp. Mol. Med.* **31,** 42–46 CrossRef Medline

48. Wang, L., Lee, G., Kuei, C., Yao, X., Harrington, A., Bonaventure, P., Lovenberg, T. W., and Liu, C. (2019) GPR139 and dopamine D2 receptor co-express in the same cells of the brain and may functionally interact. *Front. Neurosci.* **13,** 281 CrossRef Medline
49. Nepomuceno, D., Kuei, C., Dvorak, C., Lovenberg, T., Liu, C., and Bonaventure, P. (2018) Re-evaluation of adrenocorticotropic hormone and melanocyte stimulating hormone activation of GPR139 *in vitro*. *Front. Pharmacol.* **9,** 157 CrossRef Medline
50. Wang, J., Zhu, L. Y., Liu, Q., Hentzer, M., Smith, G. P., and Wang, M. W. (2015) High-throughput screening of antagonists for the orphan G-protein coupled receptor GPR139. *Acta Pharmacol. Sin.* **36,** 874–878 CrossRef Medline
51. Masuho, I., Martemyanov, K. A., and Lambert, N. A. (2015) Monitoring G protein activation in cells with BRET. *Methods Mol. Biol.* **1335,** 107–113 CrossRef Medline
52. Masuho, I., Chavali, S., Muntean, B. S., Skamangas, N. K., Simonyan, K., Patil, D. N., Kramer, G. M., Ozelius, L., Babu, M. M., and Martemyanov, K. A. (2018) Molecular deconvolution platform to establish disease mechanisms by surveying GPCR signaling. *Cell Rep.* **24,** 557–568.e5 CrossRef Medline
53. Dunn, H. A., Patil, D. N., Cao, Y., Orlandi, C., and Martemyanov, K. A. (2018) Synaptic adhesion protein ELFN1 is a selective allosteric modulator of group III metabotropic glutamate receptors in *trans*. *Proc. Natl. Acad. Sci. U. S. A.* **115,** 5022–5027 CrossRef Medline